ORIGINAL RESEARCH ARTICLE

Seeded Growth Synthesis of Uniform Gold Nanoparticles with Controlled Diameters up to 220 nm

**Hue Do Thi**[1] · **Lien Nghien Thi Ha**[2] · **Ha Chu Viet**[1]

Abstract

A method for seeded growth of particles with uniform, smooth spherical shape, and narrow size distributions is presented. By using formaldehyde (HCHO) as a reductant and without any stabilizer in an aqueous solution, gold nanoparticles with sizes up to 220 nm were prepared at room temperature. The gold nanoparticles (diameter in the range of 1–3 nm) for the first seeds are synthesized by the reduction of tetrachloroauric acid trihydrate ($HAuCl_4$) with tetrakis (hydroxymethyl) phosphonium chloride THPC ($P(CH_2OH)_4Cl$). These seeds are dispersed in the gold plating solution at pH 9.0 in the presence of HCHO. Through multi-step seeding growth, their sizes are precisely controlled just by adjusting the ratio of gold precursor to seeds. The obtained gold nanospheres are characterized by using transmission electron microscopy, a Zetasizer Nano, and UV–VIS absorption spectroscopy. This approach has excellent reproducibility and can significantly improve the monodispersity of nanospheres.

✉ Hue Do Thi
huedt@tnue.edu.vn

1 Thai Nguyen University of Education, Thai Nguyen 24000, Vietnam

2 Institute of Physics, Vietnam Academy of Science and Technology, 18 Hoang Quoc Viet, Cau Giay, Ha Noi 100000, Vietnam

Graphic abstract
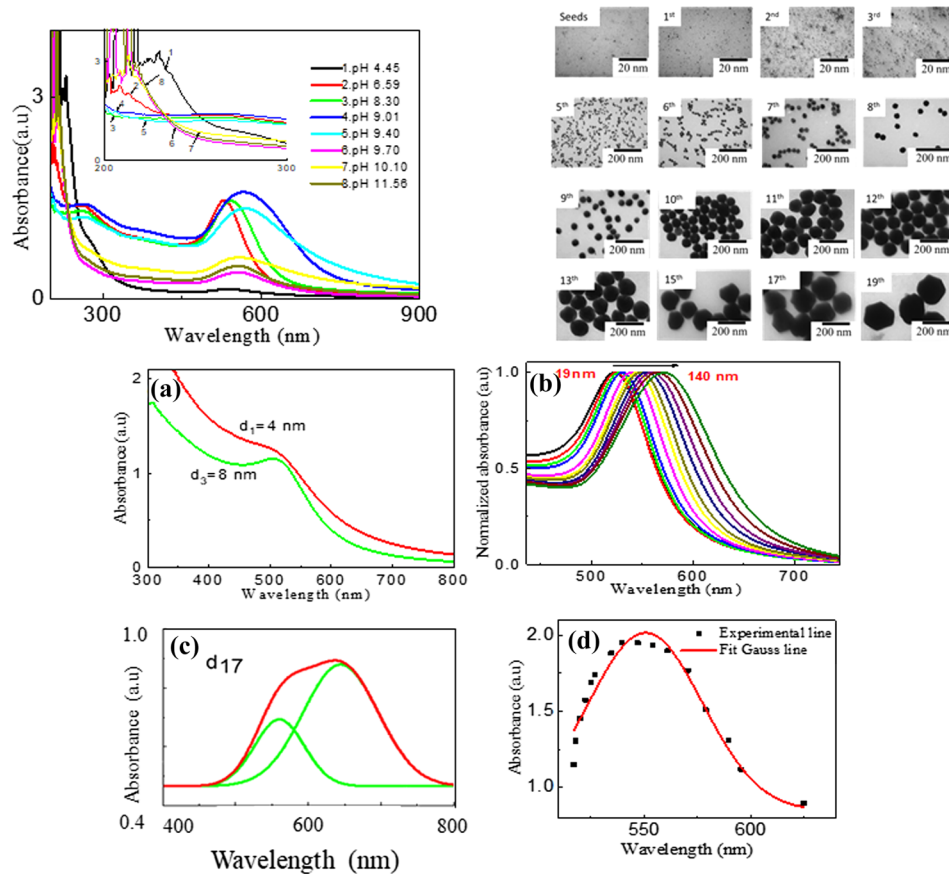
Introduction

In recent decades, gold nanoparticles (GNPs) have been attractive to many scientists in the world in different fields from fundamental research to applied research, such as photonics, electronics, catalysis, and biomedicine.[1–3] In particular, GNPs conjugated with biological elements have many applications in biology, such as labeling and imaging,[4] diagnosis, detection and treatment,[2,5] photothermal,[6,7] and distribution of biological molecules.[8,9] Also, GNPs have recently been used in advanced applications in bone tissue engineering[10] and virus detection.[11,12]

Therefore, the synthesis of GNPs has been especially studied. They can be synthesized by chemical methods by reducing the gold cations to gold atoms in the presence of a reducing agent. GNPs from 10 nm to 150 nm in diameter were prepared in one step by using trisodium citrate to reduce tetrachloroauric acid trihydrate ($HAuCl_4$).[13–16] However, the size and its distribution of the particles were not as expected, and the shapes were non-uniform when preparing

larger particles. In recent years, preparing GNPs with seeded growth approaches has been considered to be a highly effective method to create GNPs with different sizes and shapes. In the pioneering work on the citrate reduction method, Natan and co-workers reported a seeded growth using mild reducing agents, such as trisodium citrate ($Na_3C_6H_5O_7$) to prepare the GNPs up to 100 nm in diameter. However, the limitation of this method is that gold nanorods can also be formed as the second most common type of product in addition to spheres.[17] Another method has been reported by Jana et al. using cetyltrimethylammonium bromide (CTAB) as the stabilizer and sodium borohydride ($NaBH_4$) as the reductant to form GNPs from 5 nm to 40 nm in diameter.[18] With a similar idea using CTAB as the stabilizer, Murphy and Liz-Marzan controlled the seeded growth to create monodispersed GNPs up to 180 nm in diameter using ascorbic acid as the reducing agent.[19] Despite the monodispersal, these GNPs have CTAB as the surfactant cations, which limits the possibility of functionalization. This restricts the applicability of the GNPs in biomedicine. Recently, various

sized GNPs have been synthesized by a chemical reduction method with different solvent polarities.[20] However, GNPs with a diameter over 20 nm have an uneven size distribution and low synthesis efficiency, while the shape of the particles cannot be controlled. Several green methods to synthesize GNPs without adding any chemicals to the $HAuCl_4$ precursor have also been performed, but these only synthesized small GNPs (less than 50 nm).[21–24]

Hence, the detection of an efficient method leading to all the good features of the GNPs (like a large range of sizes, good size distributions, and ease of modification of the surface of the particles) is very necessary. In this study, we report a simple approach to form spherical GNPs with variable diameters ranging from 1 nm to 220 nm, monodispersed, and with high uniformity and controlled concentration. In particular, the GNPs can be easily functionalized because no CTAB molecules surround them in the growth. This method involves two stages: (1) the synthesis of the Au seeds (the GNPs with ~ 1–2 nm in diameter), and (2) the synthesis of the GNPs with variable sizes via an interparticle ripening process through multi-step seeding growth. The seeded growth was progressed by gold-plating solutions (GPS) using formaldehyde (HCHO) as a reducing reagent. The pH of the solution and the ratio of the gold precursor to the seeds ensured that the seeds were developed continuously and uniformly, and that no new particles could be formed. The size and the concentration of the particles can also be easily controlled by adjusting the ratio of the gold precursors to the seeds.

Experimental Method

Materials

Tetrachloroauric acid trihydrate ($HAuCl_4 \cdot 3H_2O$, 99.9%), trisodium citrate dihydrate ($Na_3C_6H_5O_7 \cdot 2H_2O$, 99%), potassium carbonate (99%), tetrakis (hydroxymethyl) phosphonium chloride THPC ($P(CH_2OH)_4Cl$, 80% solution in water), sodium hydroxide (NaOH, 99%), and HCHO (37% solution in water) were purchased from Merck. Deionized water was used in all the experiments. Glass containers were cleaned and dried before use.

Synthesis of GNPs up to 220 nm in Diameter

Preparation of Au Seeds (THPC–GNPs)

The Au seeds, referred to as THPC–GNPs, were prepared according to the procedure in the Ref. [25] 0.2 mL NaOH (1 M), 1.5 mL trisodium citrate (68 mM), and 0.5 mL THPC (85 mM) were added to a reaction vessel containing 21 mL water. After stirring for 5–10 min, 1 mL $HAuCl_4$ (25 mM) was added to the solution. The formation of the THPC-GNPs

was confirmed by the changing of the color from yellow to dark brown. The average diameter of the THPC–GNPs, which were stored at 4 °C before use, was determined from a transmission electron microscope (TEM; JEM 1011) image.

Preparation of Gold Plating Solutions (GPS)

The GPS must be prepared at least 3 days before the seeded growth process. The pH of the GPS was adjusted to an optimum value between 4.45 and 11.56 (value was recorded 3 days after fabrication) by changing the amount of potassium carbonate dissolved in 100 mL water. This solution was stirred for 10 min at room temperature, then 1.5 mL $HAuCl_4$ (25 mM) is added. The initial light yellow solution gradually becomes colorless after stirring for 2 h, which indicates the formation of a gold hydroxide solution (the GPS), which was stored for at least 3 days in a dark and cool area before use.

The Growth of Au Seeds

The size of the nanoparticles was estimated based on the assumption that there were no by-products in any of the growth steps, which means that the number of GNPs is equal to the number of seeds. Therefore, it is possible to approximate the size of the GNPs by using known input parameters in the following equation:

$$\frac{d_1^3}{d_2^3} = \frac{V_{seed}}{V_{GPS}} = \frac{V_{seed}}{V_{seed} + V_{GPS}} \Rightarrow d_2$$
$$= d_1 \sqrt[3]{\frac{V_{seed} + V_{GPS}}{V_{seed}}} \Rightarrow \frac{d_2}{d_1} = \sqrt[3]{\frac{V_{GPS}}{V_{seed}} + 1} \tag{1}$$

This equation is formulated under the condition that the concentration of ions Au^{3+} in the GPS equals that in the seed solution. Therefore, to be more precise, the concentration correction factor n, which is the ratio between the concentration of ions of Au^{3+} in the GPS and that in the seed solution, is added to the general case. Therefore, Eq. 1 is rewritten as follows:

$$\frac{d_2}{d_1} = \sqrt[3]{\frac{V_{GPS}}{V_{seed}} \cdot n + 1} \tag{2}$$

where d_2 is the diameter of the GNPs after a growth step, d_1 is the diameter of the seeds, V_{GPS} is the volume of the GPS, V_{seed} is the volume of the seed solution, and n is the concentration ratio of Au^{3+} in the GPS and in the seed solution. The parameter n is considered as the concentration correction factor of the ions of Au^{3+} in the GPS and in the seed solution.

A GPS with suitable pH was chosen to grow the Au seeds. A volume of the seed solution was included in the

GPS so that the volume ratio of GPS and seed solution satisfied Eq. 2. At room temperature, the size of the seeds is increased after each growth step in which the product of the previous step will be used as the seeds for the following growth step. In each step, the volume of the seeds is changed while the volume of the GPS and the HCHO is fixed at 6 mL and 5 μL, respectively. Namely, step 1: 4 mL of the Au seed solution was injected into 6 mL of the GPS while stirring (time delay ~ 5 min); then, we add 5 μL of HCHO into that solution to activate the reduced reaction. The stirring process is continued until the solution is not discolored. The volumes of the used seeds are 4 mL, 8 mL, 8 mL, 12 mL, 4 mL, 8 mL, 12 mL, and 16 mL in 8 initial steps, and 17 mL in the others, respectively. The time of a growth step is approximately 30 min. It should be noted that this process is repeated until the 20th step.
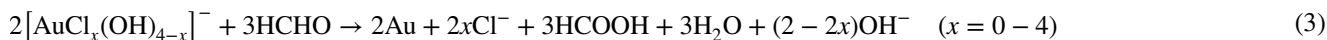
Characterization Methods

The absorption spectra were recorded on a Jasco V-570 UV–VIS/NIR spectrophotometer (200–1100 nm). The TEM images of the GNPs were obtained on a JEOL JEM 1011 microscope at an acceleration voltage of 80 kV. The polydispersity index (PDI) values and the average sizes of the GNPs were measured by a dynamic light scattering (DLS) technique with a scattering angle of 173° (Nano ZS; Malvern).

Results and Discussion

Survey of the Rate of the Reduction Reaction of HCHO in GPSs with Different pH

Similar to the synthesis of nanogold directly from the removal of Au^{3+}, the seeded growth method also strongly

Fig. 1 The absorption spectra of the GPSs with different pH values obtained about 5 min after the reduction reaction without the seeds. Inset the absorption spectra of the solutions recorded in the wavelength range from 200 nm to 300 nm.

ion complexes, as reported in previous works.[26,27] Thus, the lower the absorption intensity of the solution in the ultraviolet region, the faster the consumption rate of the gold ion complexes in the solution. As shown in the inset of Fig. 1, in the ultraviolet region, the absorption intensities of solutions with pH $\leq$ 6.59 and pH $\geq$ 9.7 are much higher than those with pH ranging from 8.3 to 9.4. These results indicate that the reduction reaction rate and the number of Au atoms formed in solutions with 8.3 $\leq$ pH $\leq$ 9.4 in the initial stage is much faster and larger than those in solutions with other pH values, respectively. This phenomenon is well known and described clearly in Ref. 28, where the dependence of the reduction reaction for HCHO on the pH of the GPS can be expressed by Eq. 3:

$$2\left[AuCl_x(OH)_{4-x}\right]^- + 3HCHO \rightarrow 2Au + 2xCl^- + 3HCOOH + 3H_2O + (2-2x)OH^- \quad (x = 0-4) \tag{3}$$

depends on the pH of the solution. Thus, the most important part of this method is to control the pH of the GPS to ensure that the seeds are developed uniformly. To find the pH value of the GPS fitting for the seeded growth process, we have investigated the effect of the pH of the GPS on the rate of reduction reaction of gold ion complexes with HCHO which occurs according to Eq. 3. The recorded pH values of the GPSs (after 3 days of preparation) are 4.45, 6.59, 6.82, 8.30, 9.01, 9.40, 9.70, 9.80, 10.10, and 11.56. Figure 1 presents the absorption spectra of the GPSs with different pH values, which are obtained about 5 min after the reduction reaction without the seeds. The absorbance in the 200–300 nm ultraviolet region is mainly due to the contribution of gold
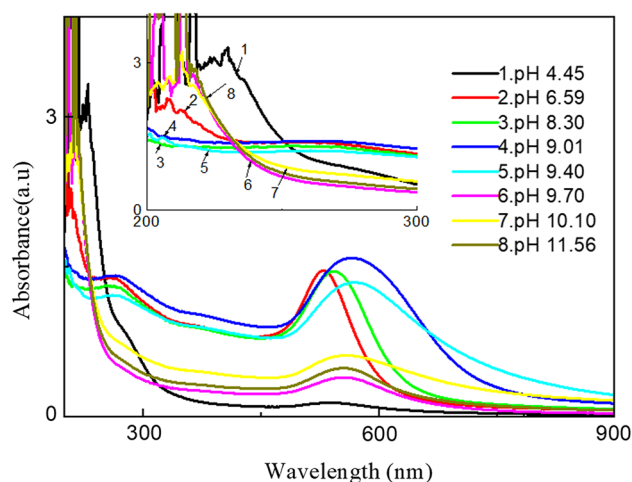
The seeded growth mechanism can be explained as follows: when the pH of the solution is below 8.3 (according to the above survey), the rate of consumption of gold ion complexes is slow, leading to the slow formation speed of Au atoms. Therefore, in the first stage, the solution has many gold ion complexes and the particle size distribution is broadened. The formation of particles in these solutions can be described through the following stages. Initially, the solution can form the new nucleus (Lamer burst nucleation[29,30]), then a random combination (random attachment[29]) occurs with the seeds. Finally, the seeds grow by the "intraparticle ripening" mechanism.[29] Under the influence of $[AuCl_4]^-$, the new nucleus, which moves from one side to the other

side, is prioritized on a crystal surface. This phenomenon induces the development of incoherence and heterogeneity of the seeds.

Figure 2 illustrates the growth of the seeds depending on the pH of the GPS: when the pH of the solution increases, the consumption rate of the gold ion complexes is fast (even in the early stage of the reaction, the concentration of gold ion complexes is very low). Consequently, the monomer concentration in these stages of the reaction increases. According to the Ostwald ripening mechanism,[29,30] the particles in the solution tend to change, so that the total surface area of them is the smallest. Thus, large particles are more stable than small particles. The small particles may clump and even disappear in the solution. When the monomer concentration in the solution reaches the saturation state, the monomers will condense on the surface of the large particles continuously and homogeneously. Consequently, the larger particles are formed uniformly in size and shape. However, when the pH of GPS is above 9.7 ($[OH^-] > 5 \times 10^{-5}$ M), the reaction of HCHO with OH^-, which is called the Cannizzaro, is given by:

$$2HCHO + 2OH^- \rightarrow HCOO^- + HCH_2O^- + H_2O \qquad (4)$$
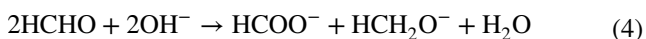
Therefore, when the pH is too high, Eqs. 3 and 4 occur simultaneously, and the reduction reaction occurs more slowly. These results reduce the rate of formation of the monomers in solution. Thus, the GPS with a pH value in the range of 8.3–9.4 is suitable for the development of the seeds. In our study, we used the GPS at pH 9.0 to grow the small gold particles.

Seeded Growth Synthesis of GNPs of up to 220 nm

Figure 3 shows the TEM image and the UV–VIS absorption spectra of the gold seeds. The morphologic properties of ultrafine GNPs are shown on the TEM image with the magnification of ×10,000. The size of the seeds is determined in a range of 1–2 nm. These seeds are also proved to be relatively stable in the trisodium citrate dihydrate buffer via UV–VIS spectra of the solution after 1 day and 30 days (Fig. 3b).

These GNPs are used as the seeds to grow into larger particles, as mentioned in the experimental section. Figure 4 shows the morphological characterization of GNPs obtained after different growth steps. The size of the GNPs is increased from 1 nm to 220 nm after the consecutive growth steps to obtain GNPs with different diameters. In addition, the optical properties of the GNPs solutions are measured by
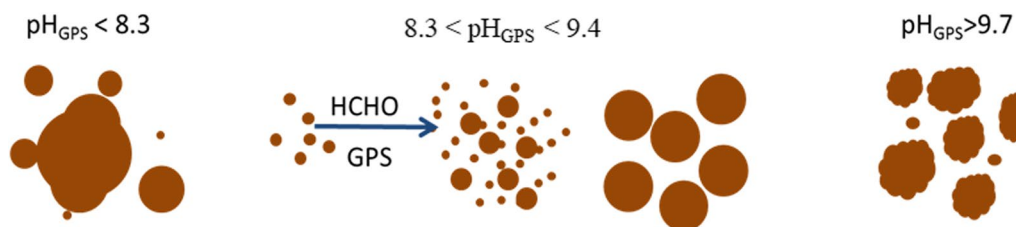

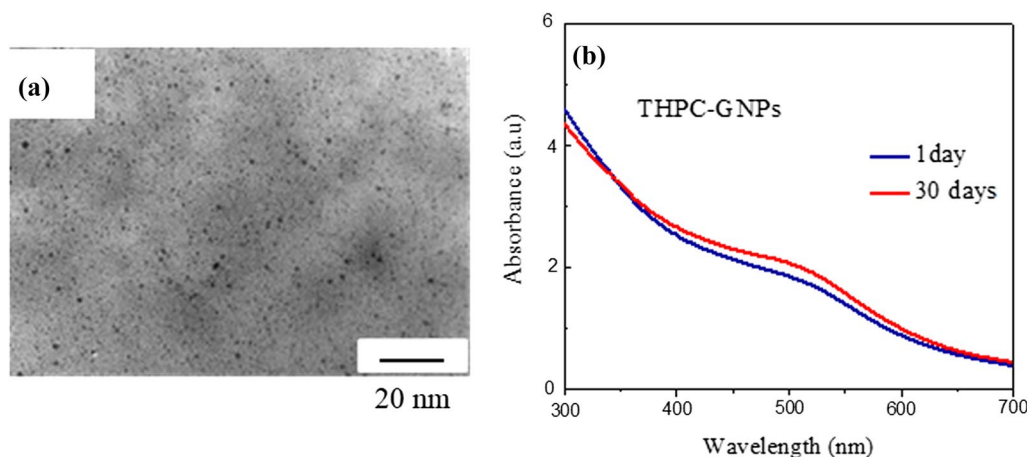**Fig. 2** The growth of the seeds depending on the pH of GPS.

Fig. 3 The TEM image of THPC–GNPs prepared in a trisodium citrate dihydrate buffer solution at 1 day after synthesis; scale bar 20 nm (a), and plasmon absorption spectra of THPC–gold solution measured after (blue line) 1 day and (red line) 30 days of preparation (b).
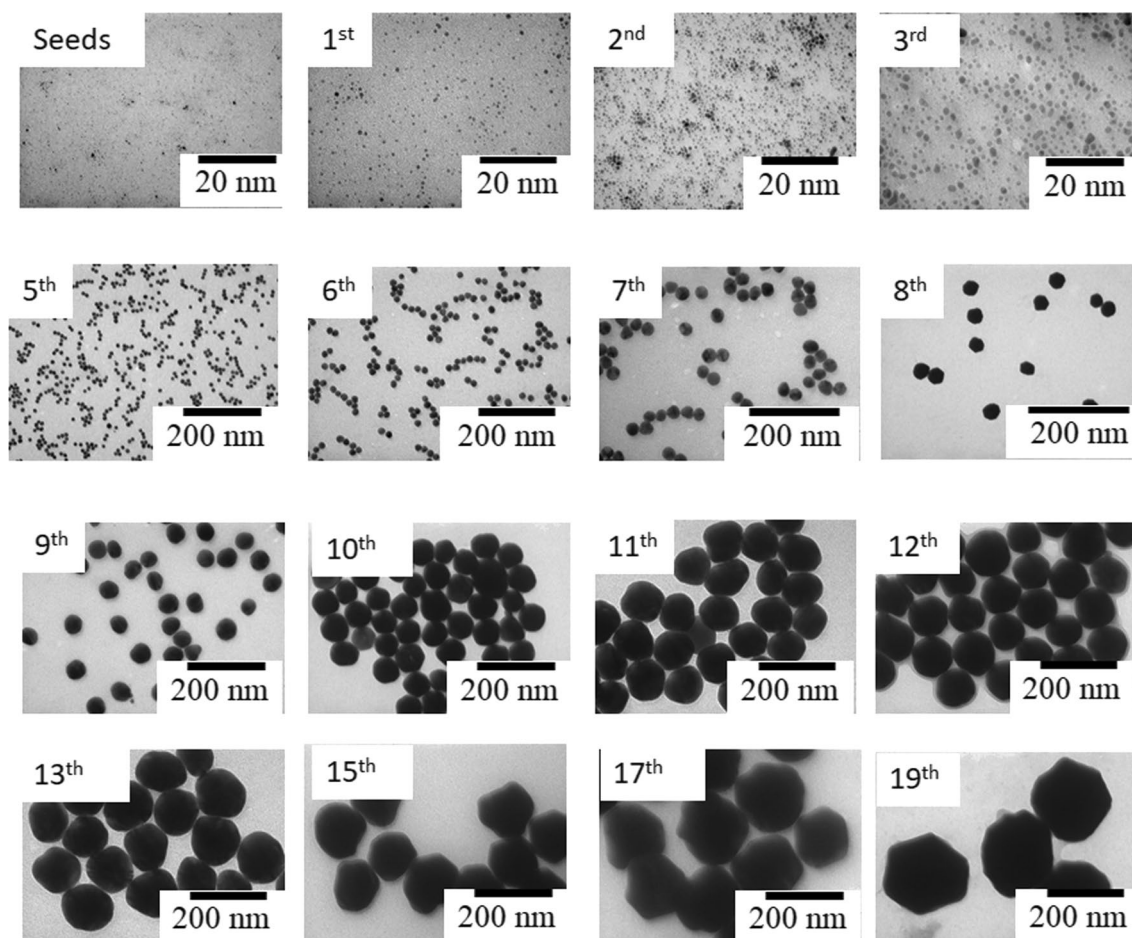
Fig. 4 Transmission electron microscopy images of Au seed particles and those obtained after different growth steps.

UV–VIS spectroscopy, as illustrated in Fig. 5. In all cases, it can be seen that the plasmon absorption spectra are symmetric, the respective wavelengths of absorbance maxima are red-shifted, and the absorption intensity depends on the respective wavelength as the Gaussian function (Fig. 5d). Interestingly, the size of the GNPs, which is measured from the TEM images after different growth steps, can be estimated by Eq. 2. This suggests that the size of the GNPs can be controlled by changing the ratio of the volume of the GPS and the seed solution.

For the optical parameters, the size of the particles is obtained from the TEM images, as well as being estimated from Eq. 2, and the particle concentrations are listed in Table I. It can be seen that the calculated particle size is in good agreement with the measured results (TEM and DLS), and that the measurements of particle size distributions indicates that the GNPs are well dispersed, and that the particle size distribution is convergent.

Conclusions

Using a simple method of seed-mediated growth, we successfully synthesized and investigated the optical properties of gold nanospheres. The synthesized spherical GNPs are relatively uniform and monodispersed, and different sizes of GNPs are controlled in the range from 1 nm to 220 nm. The mechanism of the synthesis approach is the use of HCHO as a reducing agent to reduce Au^{3+} in gold hydroxide solution to Au atoms, leading to the increase of seed size. Gold nanospheres with an average diameter of about 1–2 nm dispersed in trisodium citrate dihydrate solution were used as seeds for the first growth step. Subsequent growth steps used the product of the previous step as seeds to form larger GNPs. The seeds were grown in the GPS solution with an optimum pH 9.0. The advantage of this method is that the GNPs are made in room temperature conditions, limiting the impact of temperature on the quality of the samples. Another important point is that citrate-stabilized GNPs allow the expansion of the well-known applicability, especially in biological and biomedical applications.
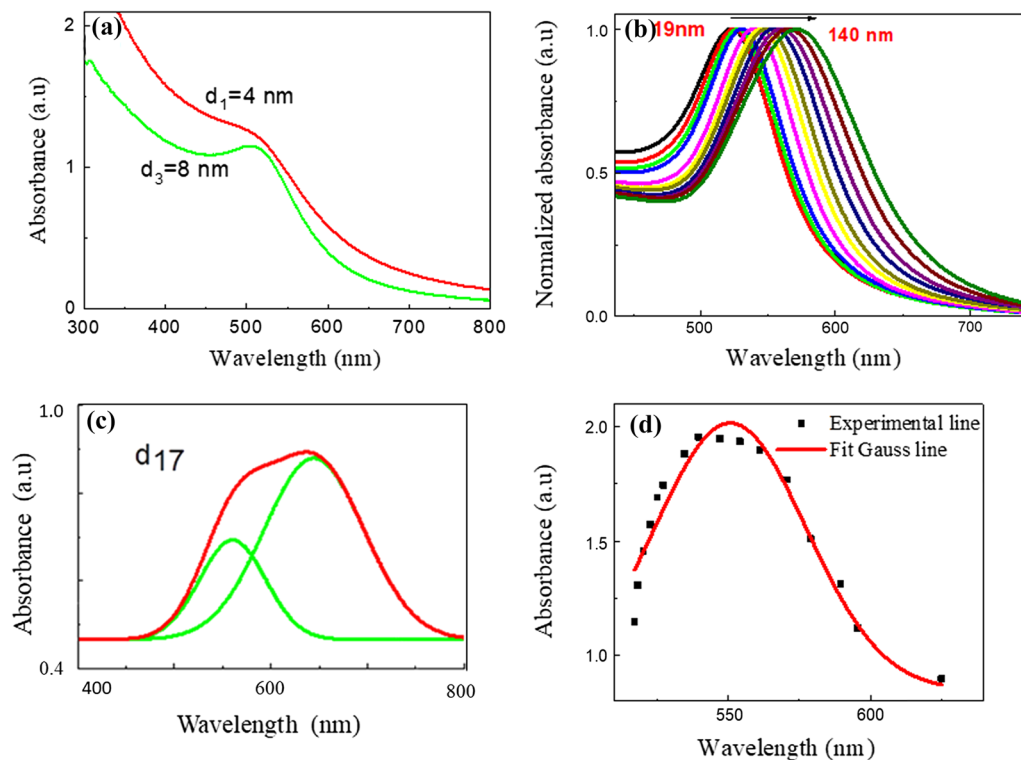
Fig. 5 Plasmon absorption spectra of gold colloids obtained after different growth steps (a–c), and absorption maximum depending on the respective wavelength fit under the Gaussian function (d).

Table I Summary of sizes, concentrations, and optical properties of the GNPs obtained after different growth steps

Growth step	Calculated diameter (nm)	SRP peak dipolar (nm)	SRP peak quadru-polar	OD	Concentration (ml^{-1})	TEM diameter (nm)	Zetasizer diameter (nm)	PDI
5	25.36	518	–	1.3	2.0×10^{11}	25 ± 1.8	28.54	0.3
7	30.56	520	–	1.4	1.1×10^{11}	30 ± 2.0	30.59	0.2
9	46.88	527	–	1.7	3.0×10^{10}	45 ± 2.5	48.36	0.2
11	70.15	547	–	1.9	0.9×10^{10}	70 ± 3.1	75.01	0.3
13	85.81	561	–	1.9	0.5×10^{10}	85 ± 3.3	90.20	0.3
14	94.91	570	–	1.8	0.4×10^{10}	95 ± 3.4	95.94	0.1
16	140.02	625	–	0.9	1.2×10^{9}	143 ± 4.2	157.8	0.03
17	157.08	544	636	0.7	8.7×10^{8}	155 ± 4.2	160.3	0.08
19	192.15	559	732	0.5	4.7×10^{8}	190 ± 4.5	219.5	0.15

References

1. K. Mahato, S. Nagpal, M.A. Shah, A. Srivastava, P.K. Maurya, S. Roy, A. Jaiswal, R. Singh, and P. Chandra, *3 Biotech* 9, 57 (2019).
2. X. Bai, Y. Wang, Z. Song, Y. Feng, Y. Chen, D. Zhang, and L. Feng, *Int. J. Mol. Sci.* 21, 2480 (2020).
3. L.H. Madkour, *Pharm. Pharmacol. Int. J.* 6, 157 (2018).
4. K. Rajesh, N. Sahithi, R. Arpita, C.Y. Hari, M. Sudip, H. Shagufta, and R.P. Chitta, *ACS Biomater. Sci. Eng* 5, 5439 (2019).
5. B. Salman, Y. Maryam, S.Q. Elmira, R. Jamal, A. Morteza, H. Mahmoud, A.M. Seyed, and K. Hamid, *Nanomed. Biotechnol.* 46, 462 (2018).

6. H. Park, D. Lim, J. Vines, J. Yoon, and N. Ryu, *Front. Chem.* 7, 001667 (2019).

7. Z. Dan, W. Tingting, Q. Xianya, Q. Qi, S. Lihuan, S. Qingle, Y. Conglian, and Z. Zhiping, *Nano Lett.* 19, 6635 (2019).

8. S. Rana, A. Bajaj, R. Mout, and V.M. Rotello, *Adv. Drug Deliv. Rev.* 64, 200 (2012).

9. S.J. Amina, and B.A. Guo, *Int. J. Nanomed.* 15, 9823 (2020).

10. H. Li, S. Pan, P. Xia, Y. Chang, C. Fu, W. Kong, Z. Yu, K. Wang, X. Yang, and Z. Qi, *J. Biol. Eng.* 14, 14 (2020).

11. M.S. Draz, and H. Shafiee, *Theranostics.* 8, 1985 (2018).

12. A.M.V. Mayra, M.S. Karla, J.M.S. Juan, R.L. Raúl, A.G.N. Marco, R.P. Cristina, G.Z.T. Diana, and M.T.Á. Laura, *Viruses* 11, 1111 (2019).

13. J. Turkevich, P.C. Stevenson, and J. Hillier, *Discuss. Faraday Soc.* 11, 55 (1951).

14. G. Frens, *Nat. Phys. Science* 241, 20 (1973).

15. A. Emmanuel, P. Luca, G. Asterios, and M. Luca, *Chem. Eng. Sci.* 191, 318 (2018).

16. J. Dong, P.L. Carpinone, G. Pyrgiotakis, P. Demokritou, and B.M. Moudgil, *Kona Powder Part. J.* 37, 224 (2020).

17. K.R. Brown, D.G. Walter, and M.J. Natan, *Chem. Mater.* 12, 306 (2000).

18. N.R. Jana, L. Gearheart, and J. Murphy, *Langmuir* 17, 6782 (2001).

19. J.R. Fernández, J.P. Juste, F.J.G. Abajo, and L.M.L. Marzán, *Langmuir* 22, 7007 (2006).

20. M.H. Hussain, N.F. Abu Bakar, A.N. Mustapa, K.F. Low, N.H. Othman, and F. Adam, *Nanoscale Res. Lett.* 15, 140 (2020).

21. B. Wang, G. Yang, J. Chen, and G. Fang, *Nanomaterials* 10, 2020 (1869).

22. O.S. ElMitwalli, O.A. Barakat, R.M. Daoud, S. Akhtar, and F.Z. Henari, *J Nanopart Res.* 22, 309 (2020).

23. L.C. Henríquez, K.A. Aguilar, J.U. Álvarez, L.V. Fernández, G.M.O. Vásquez, and J.R.V. Baudrit, *Nanomaterials* 10, 1763 (2020).

24. E.H. Ismail, A.M.A. Saqer, E. Assirey, A. Naqvi, and R.M. Okasha, *Int J Mol Sci.* 19, 2612 (2018).

25. D.G. Duff, A. Baiker, and P.P. Edwards, *Langmuir* 9, 2301 (1993).

26. Z. Liang, Y. Liu, S.S. Ng, X. Li, L. Lai, S. Luo, and S. Liu, *J. Nanoparticle Res.* 13, 3301 (2011).

27. A. Annur, S.J. Santosa, and N.H. Aprilita, *Orient J Chem.* 34, 5 (2018).

28. G.O. Mallory and J.B. Hajdu. *Electroless Plating: Fundamentals and Application* (American Electroplaters and Surface Finishers Society, 1990)

29. N.T.K. Thanh, N. Maclean, and S. Mahiddine, *Chem. Rev.* 114, 7610 (2014).

30. C.B. Whitehead, S. Özkar, and R.G. Finke, *Chem. Mater.* 31, 7116 (2019).